

# Space-time Thermodynamics of the Glass Transition

Mauro Merolle,<sup>1</sup> Juan P. Garrahan,<sup>2</sup> and David Chandler<sup>1</sup>

<sup>1</sup>*Department of Chemistry, University of California, Berkeley, CA 94720-1460*

<sup>2</sup>*School of Physics and Astronomy, University of Nottingham, Nottingham, NG7 2RD, UK*

(Dated: February 23, 2019)

We consider the probability distribution for the fluctuations in the dynamical action of glass forming materials. We argue that the so-called glass transition is a manifestation of low action tails in these distributions where the entropy of trajectory space is sub-extensive in time. These low action tails are a consequence of dynamic heterogeneity and an indication of phase coexistence in trajectory space. The glass transition, where the system falls out of equilibrium, is then an order-disorder phenomenon in space-time occurring at a temperature  $T_g$  which is a weak function of measurement time. We illustrate our perspective ideas with facilitated lattice models, and note how these ideas apply more generally.

PACS numbers: 64.60.Cn, 47.20.Bp, 47.54.+r, 05.45.-a

A glass transition, where a super-cooled fluid falls out of equilibrium, is irreversible and a consequence of experimental protocols, such as the time scale over which the system is prepared, and the time scale over which its properties are observed (for reviews see [1]). It is thus not a transition in a traditional thermodynamic sense. Nevertheless, the phenomenon is relatively precipitous, and the thermodynamic conditions at which it occurs depend only weakly on preparation and measurement times. In this Letter, we offer an explanation of this behavior in terms of a thermodynamics of trajectory space.

Our considerations seem relatively general as they are a direct consequence of dynamic heterogeneity [2] in glass forming materials, but to be explicit below we focus on kinetically constrained models [3]. We study in detail the probability distribution of the dynamical action of trajectories. We show that due to the emergence of spatial correlations in the dynamics [4], i.e. dynamic heterogeneity, these distributions have larger low action tails than what would be expected in a homogeneous system. These tails indicate a coexistence between space-time regions where dynamics is plentiful and regions where dynamics is scarce. In the latter the entropy of trajectories is subextensive in time. The glass transition, where the system falls out of equilibrium at long but finite observation time, is thus a disorder-order transition in space-time. This ordering in trajectory space is not a consequence of any underlying static transition [5]. Further, the exponential tails observed in the aging of soft materials, so-called intermittency [6], are a consequence of dynamic heterogeneity and should be seen in mesoscopic measurements in the equilibrium dynamics of glass formers.

In order to illustrate our ideas we consider two facilitated models of glass formers. One is the lattice model of Fredrickson and Andersen (FA) [7] in spatial dimension  $d = 1$ . The other is the dynamically asymmetric variant of this FA model, called the East model [8]. The FA and East models serve as caricatures of strong and fragile glass formers, respectively [9]. In both cases, there is an energy function  $J \sum_i n_i$ , where  $J > 0$  sets the equilibrium temperature scale,  $n_i$  is either 1 or 0, indicating

whether lattice site  $i$  is excited or not, and the sum over  $i$  extends over lattice sites. For the FA model, the system moves stochastically from one micro-state to another through a sequence of single cell moves, where the state of cell  $i$  at time slice  $t + 1$ ,  $n_{i,t+1}$ , can differ from that at time slice  $t$ ,  $n_{i,t}$ , only if at least one of two nearest neighbors,  $i \pm 1$ , is excited at time  $t$ . For the East model, the dynamic rules are similar, but in this case,  $n_{i,t}$  can change only if  $n_{i+1,t} = 1$ . The state of the other nearest neighbor,  $n_{i-1,t}$ , has no facilitating effect. For both models, the dynamics is time-reversal symmetric and obeys detailed balance. The equilibrium concentration of excitations,  $c \equiv \langle n \rangle = e^{-J/T}/(1 + e^{-J/T})$ , is the relevant control parameter. The average distance between excitations sets the characteristic lengthscale for relaxation,  $\ell \approx c^{-1}$ , and thus the typical relaxation time,  $\tau \approx c^{-\Delta}$ , where  $\Delta = 3$  for the FA model and  $\Delta \approx \ln c / \ln 2$  for the East model. See Ref. [3] for details.

The constraints limiting changes of  $n_{i,t}$ 's modify the metric of motion and confine the space-time volume available for trajectories [10]. This confinement of trajectory space is imagined to mimic the effects of complicated intermolecular potentials in a dense nearly jammed material. Excitations in this picture are regions of space-time where molecules are unjammed and exhibit mobility. As such, we refer to  $n_{i,t}$  as the mobility field.

The total system under consideration has  $N_{\text{tot}}$  sites and evolves for  $\mathcal{T}_{\text{tot}}$  time steps, so that the total space-time volume is  $N_{\text{tot}} \times \mathcal{T}_{\text{tot}}$ . Within it, we consider a subsystem with spatial volume  $N$ , and time duration  $\mathcal{T}$ , and use  $x(\mathcal{T})$  to denote a trajectory in that space-time volume. For the FA and East models, this trajectory specifies the mobility field  $n_{i,t}$  for  $1 \leq i \leq N$  and  $0 \leq t \leq \mathcal{T} - 1$ . The probability density functional for  $x(\mathcal{T})$ , denoted by  $P[x(\mathcal{T})]$ , defines an action,  $\mathcal{E}[x(\mathcal{T})]$ ; namely,  $P[x(\mathcal{T})] \equiv \exp(-\mathcal{E}[x(\mathcal{T})])$ . In the FA and East models,  $\mathcal{E}[x(\mathcal{T})]$  is a sum over  $i$  and  $t$  of terms coupling  $n_{i,t}$  to mobility fields at nearby space-time points [11]. As such, its average value will be extensive in  $N \times \mathcal{T}$ . This extensivity is a general property for any system with Markovian dynamics and short-ranged interparticle

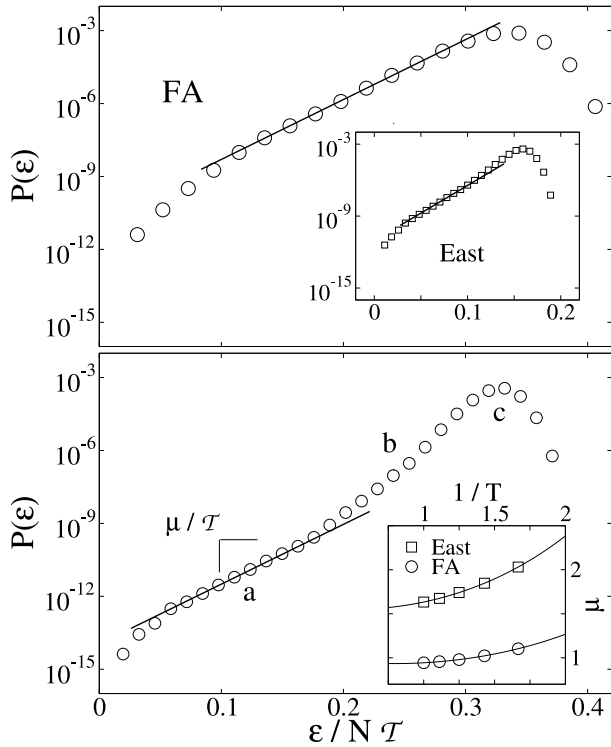


FIG. 1: Probability distribution of the action  $P(\mathcal{E})$  in the FA and East models at  $T = 1$  and subsystem size  $N = 60 \approx 16 \ell$ . (Top) FA model,  $\mathcal{T} = 320 \approx 3\tau$ . Inset: East model,  $\mathcal{T} = 1660$ . (Bottom) FA model,  $\mathcal{T} = 1280 \approx 12\tau$ . The straight lines in top and bottom panels indicate the time independent exponential tail  $\exp(\mathcal{E}\mu/t)$  (regime *a*, see text). Inset: coefficient  $\mu$  at different  $T$  from simulation and theory.

forces.

The distribution function for the action is

$$P(\mathcal{E}) = \langle \delta(\mathcal{E} - \mathcal{E}[x(\mathcal{T})]) \rangle = \Omega(\mathcal{E}) \exp(-\mathcal{E}), \quad (1)$$

where the pointed brackets indicate average over the ensemble of trajectories of length  $\mathcal{T}$ , and  $\Omega(\mathcal{E}) = \Omega(\mathcal{E}; N, \mathcal{T})$  is the number of such trajectories with action  $\mathcal{E}$ . When  $N$  is much larger than any dynamically correlated volume in space, and  $\mathcal{T}$  is much larger than any correlated period of time,

$$\ln \Omega(\mathcal{E}, N, \mathcal{T}) \equiv s(\mathcal{E}; N, \mathcal{T}) N \mathcal{T}, \quad (2)$$

will be extensive in the space-time volume  $N \mathcal{T}$ . In this case, the entropy per space-time point,  $s(\mathcal{E}; N, \mathcal{T})$ , will be intensive. Similarly, and for the same reasons, the mean square fluctuation,  $\chi(N, \mathcal{T}) = \langle \mathcal{E}^2 \rangle - \langle \mathcal{E} \rangle^2$ , is extensive for large enough  $N \mathcal{T}$ . The onset of this extensivity with respect to  $\mathcal{T}$  can be viewed as an order-disorder phenomenon, as we will discuss shortly.

The distribution function for the action can be obtained from simulation by running trajectories and creating a histogram for the logarithm of the probabilities for taking steps in the trajectory. Far into the wings of the distribution, satisfactory statistics is obtained with

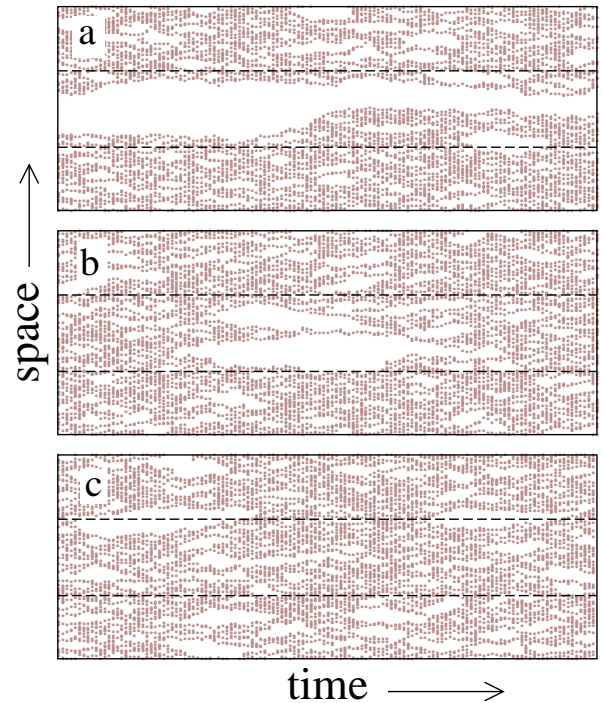


FIG. 2: Trajectories in the FA model corresponding to the regimes (a), (b) and (c) of Fig. 1(bottom). Unexcited and excited sites are coloured white and dark, respectively. Space runs along the vertical direction, and time along the horizontal direction. All panels show 200 spacial sites. Dashed lines delimit the measured space-time volume,  $N \times \mathcal{T}$ .

transition path sampling [12]. This methodology allows us to carry out umbrella sampling [13] applied to trajectory space. Figure 1 illustrates the  $P(\mathcal{E})$ 's we have obtained in this way for the FA and East models. While the bulk of the distributions is Gaussian, for values of the action sufficiently smaller than  $\langle \mathcal{E} \rangle$  they display exponential tails. Figure 2 makes vivid the fact that these tails are manifestations of dynamic heterogeneity.

The extended bubble or stripe viewed in Fig. 2(a) illustrates a volume of space-time that is absent of excitations. Because it extends throughout the pictured time frame, the statistical weight for this excitation void is dominated by the probability to observe this void at the initial time  $t = 0$ . As excitations at a given time slice are uncorrelated, this probability is Poissonian,  $\exp(-cL)$ , where  $L$  is the width of the stripe. In the presence of a bubble occupying a space-time volume  $L \mathcal{T}$ , the net action is  $\mathcal{E} \approx \mathcal{T}(N - L) \varepsilon$ , where  $\varepsilon$  is the average action per unit space-time. In this regime, the probability density for the action is then  $\exp[-cL(\mathcal{E})] \propto \exp(c \mathcal{E}/\mathcal{T}\varepsilon)$ . This proportionality explains why the slope of the exponential tail scales linearly with inverse time. The specific value of that slope is determined from evaluating the action density. Performing the requisite average of the action [11] gives  $\varepsilon \equiv \langle \mathcal{E} \rangle/N \mathcal{T} \approx -f(c) c \ln c$ , for small  $c$ , where  $f(c) \approx 2c$  for the FA model, and  $f(c) \approx c$  for the East model. Hence, to the degree that this picture is correct,

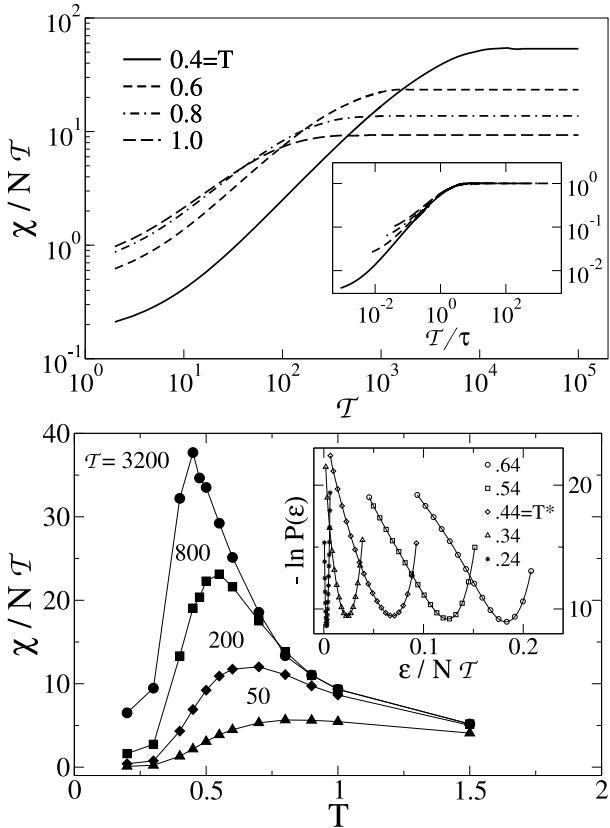


FIG. 3: (Top) Action susceptibility per unit length and time,  $\chi/N\tau$ , as a function of observation time  $\tau$  for constant temperature  $T$ , in the FA model. Inset: scaled susceptibility,  $(\tau^{-1}\chi)/[\lim_{\tau \rightarrow \infty}(\tau^{-1}\chi)]$  as a function of  $\tau/\tau$ . (Bottom) Action susceptibility per unit length and time,  $\chi/N\tau$ , but now as a function of  $T$  at constant  $\tau$ . Inset: Free energies of trajectories,  $-\ln P(\mathcal{E})$ , for observation time  $\tau = 3200$  at different temperatures. System sizes are  $N = 16c^{-1}$ . For this time  $T^* \approx 0.44$ .

the slope  $\mu/\tau$  in Fig. 1 should coincide with  $\mu = c/\varepsilon$ . The inset to Fig. 1(bottom) shows that this relationship holds to a good approximation. Thus, the exponential tail in  $P(\mathcal{E})$  manifests structures in space-time that depend upon initial conditions over a time frame  $\tau$ . It also follows that the entropy for trajectories with action that falls in the exponential tails is non-extensive in time  $\tau$ .

The tails in  $P(\mathcal{E})$  are statistically negligible when  $\tau$  is large compared to the relaxation time  $\tau$ , but they are dominant when  $\tau \lesssim \tau$ . The latter regime is where the mean square fluctuation or susceptibility,  $\chi(N, \tau)$ , is non-linear in time. Figure 3(top) shows the growth of this quantity with respect to  $\tau$ . The susceptibility per unit space-time increases with increasing  $\tau$  because increasing time allows for increased fluctuations. With the onset of decorrelation, when  $\tau > \tau$ , the susceptibility becomes extensive, and  $\chi(N, \tau)/N\tau$  becomes a constant. This plateau or constant value increases with decreasing  $T$  because fluctuations become more prevalent as  $c$  decreases. Indeed, the FA and East models approach

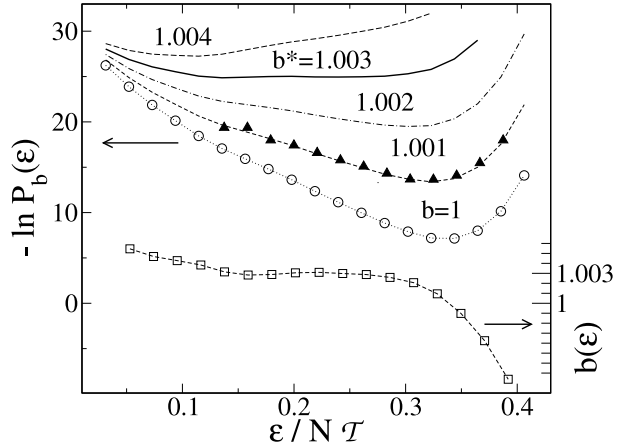


FIG. 4: Free energies of trajectories,  $-\ln P_b(\mathcal{E})$ , for different inverse dynamical temperatures  $b$ . The curve for  $b = 1$  is that of Fig. 1(a), with  $T = 1$ ,  $N = 16c^{-1}$ ,  $\tau = 320$ . The curves with  $b = 1.001, 1.002, 1.003$  are obtained from  $P_b(\mathcal{E}) \propto P_{b=1}(\mathcal{E})e^{(1-b)\mathcal{E}}$ . We also show the free energy at  $b = 1.001$  obtained from simulation using transition path sampling [12], combined with free energy perturbation theory [13]. The lower curve is the dynamical inverse temperature  $b$  as a function of action  $\mathcal{E}$ , from Eq. (3), for this temperature and space-time volume. Coexistence takes place at  $b^* \approx 1.003$ .

dynamic criticality as  $c \rightarrow 0$  [14].

While the plateau value increases with decreasing  $T$  or  $c$ , the time for the onset to extensivity also increases. As a result,  $\chi(N, \tau)$  for a given value of  $\tau$  has a maximum at this onset time. This behavior is illustrated in Fig. 3(bottom). The extremum will approach a singularity in the limit of criticality,  $\tau \rightarrow \infty$ ,  $c \rightarrow 0$ . For  $\tau$  finite, the extremum is located at a finite temperature,  $T^*$ , namely,  $\tau(T^*) \sim \tau$ , where  $\tau(T)$  denotes the equilibrium relaxation time at the temperature  $T$ . Accordingly,  $T^*$  is a glass transition temperature. In particular, below this temperature, the system will fall out of equilibrium if observed for a time not much longer than  $\tau$ . For the Arrhenius FA model,  $\ln \tau(T) \propto 1/T$ , so that  $T^*$  in this case varies logarithmically with observation time  $\tau$ . For the super-Arrhenius East model,  $\ln \tau(T) \propto 1/T^2$ ,  $T^*$  is even more weakly dependent upon observation time, going as  $1/\sqrt{\ln \tau}$ . It is due to this weak dependence on observation time that the glass transition is very nearly a material property, being confined to a narrow range of temperatures.

Figures 1–3 refer specifically to the action,  $\mathcal{E}$ . Similar behaviors are found for other measures of dynamic activity, such as the number of transitions or kinks in a space-time volume,  $\mathcal{K} = \sum_{i,t} [n_{i,t} (1 - n_{i,t+\delta t}) + (1 - n_{i,t}) n_{i,t+\delta t}]$ . Presumably, similar behaviors will be found for corresponding quantities in a continuous atomistic system. One such quantity, with mean value proportional to the Edwards-Anderson order parameter [15], is  $Q = \sum_{j \in V} \int_0^\tau dt \exp \{ik \cdot [r_j(t) - r_j(0)]\}$ , where  $r_j(t)$  refers

to the position of the  $j$ th particle at time  $t$ , and the sum includes all those particles  $j$  that are in volume  $V$  at time 0. The wave-vector  $k$  should be small enough to ensure that variation in  $Q$  is due to diffusion of particles, not simply vibrational motion. The susceptibility for this quantity  $Q$  (or its time derivative) has been considered in atomistic simulation studies of dynamic heterogeneity [2, 14, 16].

Above  $T^*$ , the system is equilibrated and disordered with respect to order parameters like  $\mathcal{E}$  or  $\mathcal{K}$  or  $Q$ . Below  $T^*$ , the system is ordered with respect to these quantities, and the order manifests dependence upon initial conditions. In view of the anomalous behavior of  $\chi(N, \mathcal{T}; T)$  near  $T = T^*$ , this dependence can be manipulated in a fashion familiar in the context of equilibrium phase transitions. To this end, it is useful to define a dynamic inverse temperature factor

$$b \equiv \partial \ln \Omega / \partial \mathcal{E}. \quad (3)$$

It is then natural to define a modified path distribution functional,

$$P_b[x(\mathcal{T})] \equiv Z_b^{-1} \exp \{-b\mathcal{E}[x(\mathcal{T})]\}, \quad (4)$$

where  $Z_b = \int d\mathcal{E} \Omega(\mathcal{E}) e^{-b\mathcal{E}}$ . Isolated equilibrium dynamics at temperature  $T$  coincides with  $b = 1$ , at which point the partition function  $Z_b$  is unity, i.e.,  $Z_1 = 1$ . Clearly,  $\langle \mathcal{E} \rangle = -[\partial \ln Z_b / \partial b]_{b=1}$ , and  $\chi(T) =$

$[\partial^2 \ln Z_b / \partial b^2]_{b=1}$ . An extremum in  $\chi(T)$  corresponds with a rapid change in  $\langle \mathcal{E} \rangle$  with respect to  $T$ , which in turn implies a bistable free energy,  $-\ln P_b(\mathcal{E})$ , near  $b = 1$  and  $T = T^*$ .

The inset to Fig. 3(b) shows the change in the free energy of trajectories,  $-\ln P(\mathcal{E})$ , at  $b = 1$  and fixed observation time  $\mathcal{T}$ , as  $T$  decreases and crosses  $T^*$ . Figure 4 shows the change in free energy, for fixed  $T$  but now changing  $b$ . The inset gives the dynamical inverse temperature  $b(\mathcal{E})$ . Coexistence takes place at  $b^* > 1$ , the precise value depending upon  $T$  and  $\mathcal{T}$ . In the case illustrated,  $b^* = 1.003$ , very close to the physical value  $b = 1$ . The basin at low action coincides with the exponential tail and thus correlation with initial conditions throughout the observed time frame.

In an isolated system in equilibrium,  $b = 1$ , there will be a true dynamical singularity, that is a transition like the one above for  $\mathcal{T} \rightarrow \infty$ , only at  $T = 0$ : from the exponential tails of  $P(\mathcal{E})$  we know that  $b^* = 1 + \mu/\mathcal{T}$ , so that  $b^* \rightarrow 1$  when  $c \rightarrow 0$  with  $\mathcal{T}/\tau \rightarrow \text{finite}$ . An interesting question is whether it is possible to define a dynamical protocol, perhaps through some form of external driving, which would allow to tune  $b$  from  $b = 1$  to  $b = b^*$ , and thus observe this dynamical transition at  $T > 0$ .

This work was supported by the NSF, by DOE grant no. DE-FE-FG03-87ER13793, by EPSRC grants no. GR/R83712/01 and GR/S54074/01, and University of Nottingham grant no. FEF 3024.

---

[1] M.D. Ediger, C.A. Angell and S.R. Nagel, *J. Phys. Chem.* **100**, 13200 (1996); C.A. Angell, *Science* **267**, 1924 (1995); P.G. Debenedetti and F.H. Stillinger, *Nature* **410**, 259 (2001).

[2] For reviews see: H. Sillescu, *J. Non-Cryst. Solids* **243**, 81 (1999); M.D. Ediger, *Annu. Rev. Phys. Chem.* **51**, 99 (2000); S.C. Glotzer, *J. Non-Cryst. Solids*, **274**, 342 (2000); R. Richert, *J. Phys. Condens. Matter* **14**, R703 (2002).

[3] F. Ritort and P. Sollich, *Adv. Phys.* **52**, 219 (2003).

[4] J.P. Garrahan and D. Chandler, *Phys. Rev. Lett.* **89**, 035704 (2002).

[5] For thermodynamic approaches to the glass transition see e.g. D. Kivelson et al., *Physica A* **219**, 27 (1995); X. Xia and P.G. Wolynes, *Proc. Natl. Acad. Sci. USA* **97**, 2990 (2000).

[6] L. Cipelletti et al. *J. Phys. Condens. Matter* **15**, S257 (2003); L. Buisson, L. Bellon and S. Ciliberto, *ibid.*, S1163 (2003); C. Chamon, et al., *J. Chem. Phys.* **121**, 10120 (2004); F. Ritort, *cond-mat/0405707*. See also S.T. Bramwell et al., *Phys. Rev. Lett.* **84**, 3744 (2000).

[7] G.H. Fredrickson and H.C. Andersen, *Phys. Rev. Lett.* **53**, 1244 (1984).

[8] J. Jäckle and S. Eisinger, *Z. Phys. B* **84**, 115 (1991).

[9] J.P. Garrahan and D. Chandler, *Proc. Natl. Acad. Sci. USA* **100**, 9710 (2003); Y.J. Jung, J.P. Garrahan and D. Chandler, *Phys. Rev. E* **69**, 061205 (2004).

[10] S. Whitelam and J.P. Garrahan, *J. Phys. Chem. B* **108**, 6611 (2004).

[11] The action  $\mathcal{E}[x(\mathcal{T})]$  in has the form [4]:  $\mathcal{E}[x(\mathcal{T})] = \sum_{i,t} \{ \mathcal{C}_{i,t} \mathcal{E}_{i,t}^{(0)} + \Lambda(1 - \mathcal{C}_{i,t})[n_{i,t}(1 - n_{i,t+1}) + (1 - n_{i,t})n_{i,t+1}] \}$ . Here  $\mathcal{C}_i$  is the kinetic constraint,  $\mathcal{C}_{i,t} = n_{i+1,t} + n_{i-1,t} - n_{i+1,t}n_{i-1,t}$  for the FA model, and  $\mathcal{C}_{i,t} = n_{i+1,t}$  for the East model;  $\mathcal{E}_{i,t}^{(0)}$  is the unconstrained action at site  $i$ , such as  $\mathcal{E}_{i,t}^{(0)} = -n_{i,t+1} \ln c - (1 - n_{i,t+1}) \ln(1 - c)$  for Glauber dynamics; and  $\Lambda \rightarrow \infty$  imposes the kinetic constraint. In practice the action can be calculated by accumulating the logarithm of the probability of each accepted or rejected move. We use continuous time Monte Carlo where all attempted moves are accepted; see e.g. M.E.J. Newman and G.T. Barkema, *Monte Carlo Methods in Statistical Physics* (Oxford University Press, Oxford, 1999). In our simulations each spin is assigned its own clock, thus removing constant  $\ln N$  terms from the action. This feature is essential for the entropy of trajectory space to be extensive in  $N$ .

[12] P.G. Bolhuis et al., *Annu. Rev. Phys. Chem.* **59**, 291-318 (2002).

[13] D. Frenkel and B. Smidt, *Understanding Molecular Simulation* (Academic Press, Boston, 2002).

[14] S. Whitelam, L. Berthier and J.P. Garrahan, *Phys. Rev. Lett.* **92**, 185705 (2004).

[15] K.H. Fischer and J.A. Hertz, *Spin Glasses* (Cambridge University Press, Cambridge, 1993).

[16] C. Toninelli et al., *cond-mat/0412158*.